J. W. Simmelink, [1] *Ph.D.; E. M. Robinson,* [1] *D.D.S.; and*
L. S. Staikoff, [1] *B.S.*

Identification of Bullet Particles in Bone Fragments by Electron Beam X-Ray Microanalysis

ABSTRACT: Small fragments of human temporal bone from skeletal remains were examined to identify radiopaque particles associated with the bone. Scanning electron microscopy, X-ray energy dispersive analysis, and electron probe microanalysis were used in examining both external bone surfaces and the internal bone areas that were exposed by cutting sections through the bone fragments. Elemental analysis of the bone surface showed aluminum, silicon, chlorine, potassium, calcium, and iron. Electron probe X-ray mapping of radiopaque particles embedded in the bone identified lead as the major element and antimony as the minor element. This method is useful for elemental analysis of micrometre-sized particles found in or on calcified tissues.

KEYWORDS: criminalistics, ballistics, musculoskeletal system, bullet, bone, scanning electron microscopy, X-ray microanalysis

Compared to the light microscope, the scanning electron microscope (SEM), with its improved resolution, depth of focus, and ease of sample preparation, has proven an ideal instrument for the examination of the surfaces of optically opaque objects. Characteristics of bullet striations [1] and calcified tissue [2,3] have been the subjects of several SEM reports. In addition to morphological details, elemental composition of specimens can be determined by an X-ray energy dispersive detector coupled to an SEM or by electron probe microanalysis. Both have been used in the elemental analysis of microscopic samples with forensic science importance, such as paint chips [4], gunshot residue [5], and bullet particles [6].

These instruments were used in a coroner's case involving human skeletal remains in cardboard cartons that also contained damp earth, vegetation, and pieces of fabric. The bones and bone fragments were placed in anatomical arrangement, itemized, and photographed. Both physical examination and clinical X-ray examination of the skeletal remains and other material in the cartons were performed, but no bullet was found. Of particular interest to this study was a fragmented piece of the petrosal portion of the left temporal bone. The margins of a defect in this bone fragment were examined by SEM and X-ray analysis to identify small radiopaque particles associated with the bone.

Materials and Methods

Two portions (about 5 by 5 mm) of the fragment of the left temporal bone that contained the radiopaque particles were removed with a #2 round dental bur. A fine jeweler's saw may also be used for removing small pieces of bone. The isolated samples were then X-rayed (Kodak ultra-speed-D film exposed at 65 kV and 15 mA for 0.5 s), glued to aluminum sample stubs, and vacuum-coated with carbon (50 nm thick). The samples were examined in a Cambridge S4-10 SEM with a Kevex energy dispersive detector and Nuclear Data analyzer. The SEM was operated at 20 kV with the sample tilt and rotation optimized for X-ray collection. Following the microscopy and analysis of the surface of the samples, they were embedded in an epoxy resin [7] and cured for 24 h at 60°C. The embedded bone was then sliced into 200-μm-thick sections with a water-cooled saw equipped with a 76-mm-diameter by 0.38-mm-thick (3- by 0.015-in.) rubber-bonded silicon carbide wheel (Allison-Campbell Co., Shelton, Conn.). The sections were placed in sequence on X-ray film and exposed for 0.2 s at 65 kV and 15 mA (Fig. 1a). Those sections of bone that contained radiopaque particles were prepared for the SEM as previously indicated. Selected sections were also examined at 80 kV in an electron microprobe (Materials
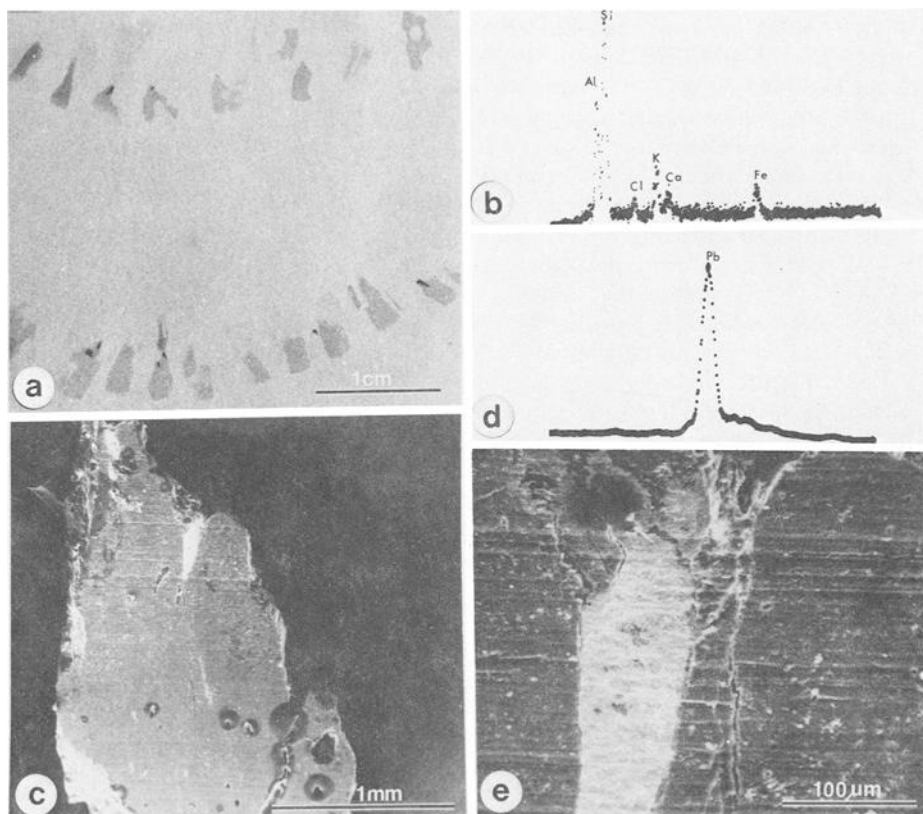
FIG. 1—(a) *X-ray of sections of bone fragments. Some of the sections show small, dark, radiopaque particles.* (b) *Energy dispersive analysis from the surface of the bone fragment.* (c) *Scanning electron micrograph of section of bone fragment containing a radiopaque particle that appears as the brighter ovoid area near the top of the bone section.* (d) *Energy dispersive analysis of the radiopaque particle embedded in the bone.* (e) *Scanning electron micrograph of section of bone fragment with the radiopaque particle in the center. This same area was used for X-ray mapping (Fig. 2).*

Analysis Co., Model 400 S). For calcium ($K\alpha_1$) and antimony ($L\alpha_1$), the lithium fluoride analyzing crystal was used, and the ammonium di-hydrogen phosphate analyzing crystal was used for the lead ($M\alpha_1$). The X-ray mapping was done at the same magnification ($\times 220$) and for the same time (5 min) for all analyzed elements.

Results and Interpretation

The surface of the bone was examined in the SEM to determine the location of the radiopaque particles and the nature of any contaminating material derived from the environment in which the bones were found. Energy dispersion analysis (Fig. 1b) showed the following keV $K\alpha_1$ peaks with the element in parenthesis: 1.48 (aluminum), 1.74 (silicon), 2.62 (chlorine), 3.31 (potassium), 3.69 (calcium), and 6.40 (iron). The calcium is due to the hydroxyapatite crystals that form the calcified portion of bone. The aluminum is from the aluminum stub that was used to mount the samples. The silicon, chlorine, potassium, and iron may be due to the sand and salts present in the soil where the bones were found. The iron may also be part of the hemoglobin from red blood cells. No lead peaks were detected by energy dispersion analysis on the bone surface.

After the surface examination, the bone samples were cut and the sections exhibiting radiopaque areas (Fig. 1a) were reexamined to analyze their cut surfaces in the SEM. The 50- to 100-μm dense areas on the clinical X-rays appeared in the SEM as regions that were brighter than the surrounding bone (Fig. 1c). The bone was compact with small vascular channels present on the cut surface. When examined by energy dispersion analysis (Fig. 1d), the bright areas showed a strong peak for lead (2.35 keV for $M\alpha_1$). It could not be determined whether antimony (3.61 keV $L\alpha_1$) was present because the calcium (3.69 keV $K\alpha_1$) in the surrounding bone had a similar kiloelectron voltage.

The same sample was analyzed in the electron microprobe. The area that was used for X-ray mapping is seen in Fig. 1e, with the brighter embedded material bisecting the central area of the micrograph. X-ray mapping for calcium (Fig. 2) matched the region of compact bone, whereas the X-ray mapping for lead showed a heavy distribution over the embedded radiopaque particle. When the electron microprobe was focused on the $L\alpha_1$ peak for antimony, a distribution was seen over the same area as that observed for lead. To show that the X-rays for antimony were significantly above background, the electron microprobe spectrometer was defocused. Figure 2, upper right, is the result and shows "background" radiation. The data presented as X-ray mapping are not strictly quantitative [8,9]; however, they demonstrate that the radiopaque particles embedded in bone are primarily lead with a small percentage of antimony.

Discussion

Radiopaque particles are usually of sufficient size, number, and density to be easily observed on clinical X-rays [10]. When these particles are seen adjacent to entrance wounds, they are automatically assumed to be bullet fragments associated with a gunshot wound. However, in cases where a bullet is not recovered and the area of the wound is altered by decomposition of the soft tissue or fragmentation of the calcified tissues, a more definitive identification of small radiopaque particles is useful to establish that they are indeed fragments of bullets.

A previous study using energy dispersive analysis has shown X-ray mapping of lead along the bony defects of an entrance wound [11], and lead has also been detected by the same method on the skin surrounding an entrance wound [12]. This study, however, is the first to report the presence of both lead and antimony in bone-embedded radiopaque particles detected by X-ray mapping analysis. The amount of antimony found is consistent with the 1 to 2% present in bullets manufactured by a variety of companies [13,14]. For
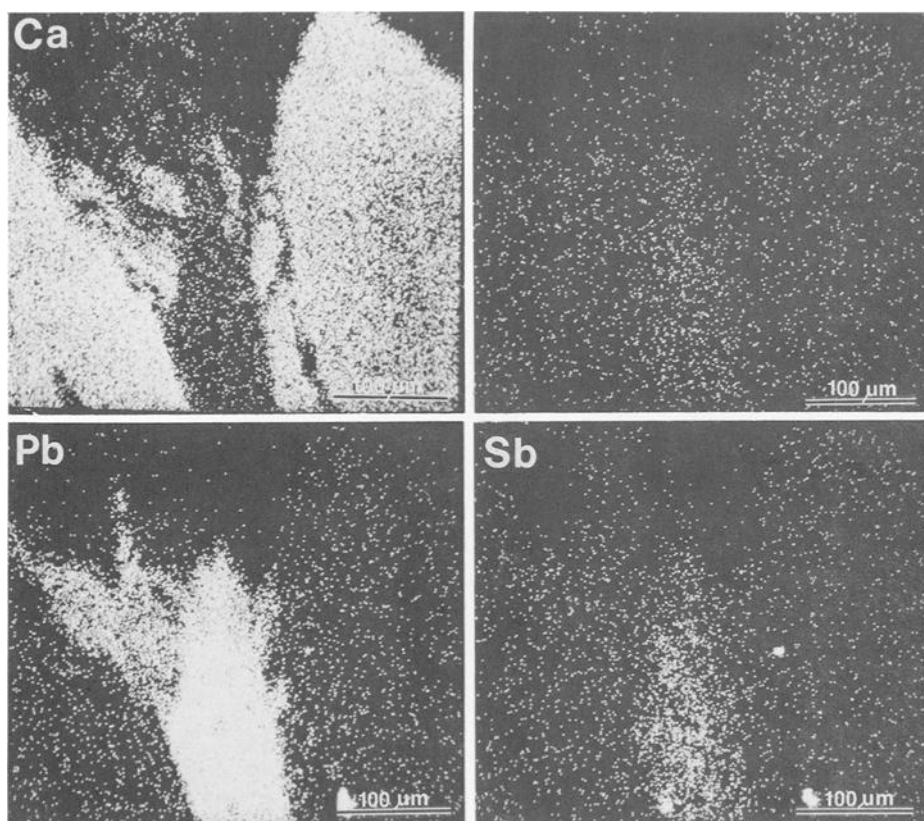
FIG. 2—*Electron probe microanalysis using X-ray mapping of area shown in Fig. 1e. The calcium (Ca) is distributed in the bone, the lead (Pb) and antimony (Sb) are distributed in the radiopaque particle; the top right section shows "background" radiation.*

some of the other trace elements (copper, tin, silver, and aluminum) found in bullets, neutron activation analysis has been effectively used [*14*], but it cannot be conveniently used to identify lead [*15*].

If only lead needs to be identified, the SEM/energy dispersive analysis is sufficient; but if antimony is to be identified, a problem exists when the bullet fragment is embedded in bone. The calcium $K\alpha_1$ (3.69 keV) and the antimony $L\alpha_1$ (3.61 keV) interfere with each other because of the relatively poor resolving power (0.15 keV) of the solid-state detectors [*9, 16*]. In this study, the electron microprobe was used for the identification of antimony because its resolution (0.015 nm) is sufficient to resolve calcium $K\alpha_1$ (0.335 nm) for antimony $L\alpha_1$ (0.343 nm).

When the radiopaque particles are very small (< 100 μm), they are difficult to distinguish on a clinical X-ray, but in the SEM they are readily located as areas brighter than the surrounding bone (Figs. 1c and e). This is due to the large difference in atomic number between the element lead and the elements calcium and phosphorus, which are the major elements in calcified tissues. Both the secondary electrons from the sample and the "back-scatter" electrons from the electron beam contribute to the elemental difference observed on the SEM micrographs [*9*].

The presentation of the electron microprobe data as X-ray mapping (Fig. 2) not only

clarifies the relative proportion of lead and antimony present, but it also characterizes their location within the calcified tissue. Further, when the elemental analysis is presented as X-ray mapping, it has additional value as evidence because it is quickly interpreted by the nonscientist, whereas kiloelectron volt numbers, wavelengths in nanometres, and graphs are often difficult to understand without extensive explanations.

Acknowledgments

References

[1] Judd, G., Sabo, J., Hamilton, W., Ferriss, S., and Horn, R., "SEM Microstriation Characterization of Bullets and Contaminant Particle Identification," *Journal of Forensic Sciences,* Vol. 19, No. 4, Oct. 1974, pp. 798-811.

[2] Johari, O. and Becker, R. P., Eds., *Scanning Electron Microscopy/1979/Part II,* Scanning Electron Microscopy, Inc., AMF O'Hare, Chicago, 1979, pp. 383-580.

[3] Vincent, J. F. V. and Currey, J. D., Eds., *The Mechanical Properties of Biological Materials,* Cambridge University Press, New York, 1980, pp. 75-168.

[4] Whitney II, W. P. and MacDonnel, H. L., "Forensic Applications of the Electron Microprobe," *Journal of Forensic Sciences,* Vol. 9, No. 4, Oct. 1964, pp. 511-519.

[5] Nesbitt, R. S., Wessel, J. E., and Jones, P. F., "Detection of Gunshot Residue by Use of the Scanning Electron Microscope," *Journal of Forensic Sciences,* Vol. 21, No. 3, July 1976, pp. 595-610.

[6] Taylor, R. L., Taylor, M. S., and Noguchi, T. T., "Application of SEM/X-ray Analysis at the Los Angeles County Forensic Science Center," in *Scanning Electron Microscopy/1975 (Part II).* O. Johari, Ed., IIT Research Institute, Chicago, 1975, pp. 494-502.

[7] Erlandson, R. A., "A New Maraglas-D.E.R. 732 Embedment for Electron Microscopy," *Journal of Cell Biology,* Vol. 22, No. 3, Sept. 1964, pp. 704-709.

[8] Edie, J. W. and Glick, P. L., "Irradiation Effects in the Electron Microprobe Quantitation of Mineralized Tissues," *Journal of Microscopy,* Vol. 117, Part 2, Nov. 1979, pp. 285-296.

[9] Heinrich, K. F. J., *Electron Beam X-ray Microanalysis,* Van Nostrand Reinhold Co., New York, 1981.

[10] Blaschke, D. D. and Sanders, B., "Radiology of Maxillofacial Gunshot Injuries," *Oral Surgery, Oral Medicine, Oral Pathology,* Vol. 47, 1979, pp. 249-299.

[11] Taylor, R. L., Taylor, M. S., and Noguchi, T. T., "Firearm Identification by Examination of Bullet Fragments: An SEM/EDS Study," in *Scanning Electron Microscopy/1979 (Part II).* O. Johari and R. P. Becker, Eds., Scanning Electron Microscopy, Inc., AMF O'Hare, Chicago, 1979, pp. 167-174.

[12] Boehm, E., "Application of the SEM in Forensic Medicine," in *Scanning Electron Microscopy/ 1971 (Part II),* O. Johari, Ed., IIT Research Institute, Chicago, 1971, pp. 553-560.

[13] Guy, R. D. and Pate, B. D., "Studies of the Trace Element Content of Bullet Lead and Jacket Material," *Journal of Forensic Sciences,* Vol. 18, No. 2, April 1973, pp. 87-92.

[14] Lukens, H. R. and Guinn, V. P., "Comparison of Bullet Lead Specimens by Nondestructive Neutron Activation Analysis," *Journal of Forensic Sciences,* Vol. 16, No. 3, July 1971, pp. 301-308.

[15] Krishnan, S. S. and Nichol, R. C., "Identification of Bullet Holes by Neutron Activation Analysis and Autoradiography," *Journal of Forensic Sciences,* Vol. 13, No. 4, Oct. 1968, pp. 519-527.

[16] Keeley, R. H. and Robeson, M. L., "The Routine Use of SEM and Electron Probe Microanalysis in Forensic Science," in *Scanning Electron Microscopy/1975 (Part II),* O. Johari, Ed., IIT Research Institute, Chicago, 1975, pp. 479-486.

Address requests for reprints or additional information to
James W. Simmelink, Ph.D.
School of Dentistry
Case Western Reserve University
Cleveland, Ohio 44106